Gloss Patch Selection based on Support Vector Regression

Chunghui Kuo, Yee Ng and C. Jeffrey Wang
NexPress Solutions LLC.
1447 St. Paul Street, Rochester, NY14653, USA

Abstract

Gloss uniformity is an important attribute affecting overall quality for reflective images. Hence, the existence of differential gloss will impair perceived image quality [1,2]. As a result, it is desirable to measure the amount of differential gloss existing on a printed image. There are two approaches to quantify the differential gloss: direct instrument measurement and indirect estimation based on a priori model [2]. In this proposal, we will adopt a support vector regression technique based on 1-norm penalty function to identify (density/gloss) patches that are important under various printing processes and paper types. As a result, these patches can be printed and measured such that a mapping function $\mathbf{f}$ can be established, which, in turns, is used to quantify the differential gloss in a printed image.

1. Introduction

In human visual perception, color, texture, shape and gloss are among important appearance attributes. Color and stereo vision are especially emphasized within the image processing and human vision research in the last several decades. However, gloss appearance and measurement are comparatively less developed and understood [3,4]. Color and gloss are appearance attributes perceived by human beings when light is cast on an object. Color information is perceived in the spectrum (frequency) domain, and the geometric properties of the object contribute to the perceived gloss. Let $L(\lambda)$ be the perceived spectrum. It is reasonable to assume that $L(\lambda)$ contains all of the color information perceived by human beings. Moreover, it was shown to be sufficient to compress $L(\lambda)$ with infinite dimensions into three dimensions [3]. Nonetheless, it is less straightforward to measure gloss. The physical properties describing interaction between incident light and the surface of an object is the *Bidirectional Reflectance Distribution Function*, *BRDF*, $\rho_{bd}(\theta_i, \phi_i, \theta_r, \phi_r)$, where angles of the incident and reflected light are denoted as (θ_i, ϕ_i) and (θ_r, ϕ_r) respectively [5]. Researchers have shown that simple algebraic equations are not adequate to explain the perceived characteristics of gloss on painted specimen [4]. Hence, this also means that it is still unclear how to reduce the number of measurement pertaining human beings' gloss perception like measuring color. R. Hunter identified six types of gloss recognizable by people, and they are: specular gloss, sheen, contrast gloss, absence-of-bloom gloss, distinctness-of-image gloss (*DOI*) and surface uniformity gloss [3].

Our objective is to identify patches with different *CMYK* compositions such that an accurate regression function correlating between toner density and visual gloss can be obtained. However, it is obvious that only parts of the listed gloss attributes are observed. For example, *DOI* rarely exists on a print. Secondly, we assume that surface uniformity gloss is insignificant in our assessment. Based on the experiment done by Hunter [3], 60-degree specular gloss measurement ranging from 15 to 80 correlates well with human beings observation. Note that the linear visual response range of 60-degree and 75-degree gloss measurement overlaps significantly, people also use 75-degree gloss reading to correlate with human visual response. Since the 60-degree gloss reading from most of our print samples also reside within this range, we adopt the 60-degree specular gloss measurement as one of the important visual gloss factors. The experiment done by F. Billmeyer and F. O'Donnell concluded that observers can only concentrate on one gloss attribute because the MDS analysis showed that there exists only one significant factor [4]. Assuming that specular gloss is the most noticeable gloss attribute, we adopt the 60-degree specular gloss measurement as the controlling parameter.

Two types of functions are used in a regression technique: global functions and local functions. The trigonometric and polynomial functions belong to the global functions where modification at a local region will influence the approximation globally. On the other hand, modifying a local function will not affect the approximation elsewhere. For example, the Fourier transform and Wavelet transform adopts global and local functions respectively [6]. In our application, the underlying physical behavior relating the amount of toner laydown and the measured gloss is still unclear. Hence, it is more appropriate to approximate the mapping function $\mathbf{f}(p_c, p_m, p_y, p_k) \approx g_{60}$ locally. As a result, there is a tradeoff between the number

of sample points and the approximation accuracy. Conceptually, we can imagine that dense sampling is needed where the curvature of the mapping function is significant. This is analogous to image compression where it was shown by Mallat that satisfactory reconstruction can be achieved by using only the local maximum of wavelet coefficients [6]. However, our problem is complicated by the amount of different printing processes and paper substrates. Assuming S represents the set containing all possible mapping functions, our proposed patch selection algorithm first adopts the singular value decomposition to approximate S by $\hat{S} \equiv Span\{v_1, v_2, \cdots, v_k\}$, where v_k represents the k-th singular vector. Then, a support vector regression technique is used to identify important patches to describe $\hat{S}$. Our experiment demonstrates that the set of selected patches successfully predict the measured gloss under different printing processes and paper substrates.

2. Support Vector Regression

The support vector machine is first developed in supervised learning by V. Vapnik [7,8]. In the simplest case, we can assume that there exists two classes of data, and they can be separated via a hyperplane. Since this hyperplane can be written as $w'x + b$, we can let $y = 1, -1$ representing the class each data belongs, and the above hyperplane separability can be shown to satisfy the following constraint [7]:

$$y_i(w'x_i + b) \geq 1. \qquad (1)$$

There are usually more than one set of solutions $[w' \quad b]^T$ satisfying the above inequality. The objective of unsupervised learning is to minimize the training error as well as the generalization error. The following theorem provides the upper bound for the classification error [7]:

Theorem Let **H** be a hyperspace having *VC* dimension d. For any probability distribution D on **X**×[-1 1], with probability $1 - \delta$ over l random examples S, any hypothesis $h \in$ **H** that makes k errors on the training set S has error no more than

$$err(h) \leq \frac{2k}{l} + \frac{4}{l}(d\log\frac{2el}{d} + \log\frac{4}{\delta}) \qquad (2)$$

provided $d \leq l$.

This theorem can be further simplified to be equal to achieving *Maximal Margin Bound*. Because only small portion of the existing data set can be separated via a hyperplane, the above derivation can be extended to a higher-order feature space via a kernel mapping function [7,8]. One advantage of this technique is that only a small subset of the original data is identified as *support vectors*, which are sufficient to construct the separating hypersurface.

Researchers have extended the support vector machine formulation to data regression [9,10,11,12]. In this paper, we basically follow the formulation proposed by Mangasarian and Musicant because of its simplicity [9]. Let the system matrix $A \in R^{l \times d}$ contain l data points in R^d, and y_i, $i = 1 \cdots l$, be a real number associated with each data point. A nonlinear kernel $K(A, A^T) : R^{l \times d} \times R^{d \times l} \longrightarrow R^{l \times l}$ is adopted. The support vector regression problem, *SVR*, can be formulated as following [9]:

$$\min_{\alpha^1, \alpha^2, b, t, \epsilon} \frac{1}{l}e'(\alpha^1 + \alpha^2) + \frac{C}{l}e't + C(1 - \mu)\epsilon \qquad (3)$$

subject to

$$K(A, A^T)(\alpha^1 - \alpha^2) + be - y \quad \leq \quad t + e\epsilon \qquad (4)$$

$$K(A, A^T)(\alpha^1 - \alpha^2) + be - y \quad \geq \quad -t - e\epsilon \qquad (5)$$

$$\alpha^1, \alpha^2, t \quad \geq \quad 0. \qquad (6)$$

$\mu \in [0\ 1]$ is an accuracy control parameter [11]. Moreover, C specifies the penalty severity applied on the regression error. Large C imposes significant penalty, which, in turns, implies that we have higher confidence on the measured data.

3. Patch Selection Algorithm

The objective of this algorithm is to construct a set $P \equiv \{p_1, p_2, \cdots p_n\}$, where $p_i = [p_c(i)\ \ p_m(i)\ \ p_y(i)\ \ p_k(i)]^T$ is crucial for building a mapping function from the toner percentage to the measured 60-degree gloss value under certain conditions. A brute force approach is to find the union of sets P^k for every possible condition. This exhaustive search is not only time consuming, but, more importantly, the union set $\tilde{P} = \bigcup_k P^k$ might contain most of the sampled patches even though we successfully reduce the number of selected patches for each P^k.

As noted previously, our patch selection problem is similar to data compression. Both goals are to reduce the number of points to satisfactorily approximate the original data. Hence, similar to data compression, we can assume that the characteristics of the mapping function f can be decomposed as following:

$$g \quad = \quad \{a\ priori\ model + residual\} + noise \qquad (7)$$

$$= \quad f + n \qquad (8)$$

where *a priori model* represents our prior knowledge about this system and the remaining information is denoted as *residual*. Assuming that *a priori model* is only controlled by a few parameters which can be easily obtained, more samples can be devoted to estimating the *residual*. This, in turns, might result in more accurate approximation with the same amount of samples.

3.1. Quadratic Mixture Model

We need to take a closer look at the physical and psychological characteristics with respect to the perceived gloss on a print. Generally, the perceived gloss is composed of wide spectrum, which means that those light does not go through the color absorbing material, i.e., toners. Therefore, we can assume that light reflected from the outmost surface contributes most of the perceived gloss. As a result, the geometric properties and the reflectance coefficient of that surface controls the perceived gloss. A rough surface will scatter more light such that a gloss meter collects less photons at the specified angle. In the mean time, the reflectance coefficient of the surface material will determine the proportion of the incident light being reflected. Under the condition that the surface material is predetermined, the geometric properties of the outmost surface alone affects the measured gloss value.

There are various types of printing processes. For example, the lithography, the ink jet printing and the electrophotography, etc.. In this paper, we will concentrate on the electrophotography which uses toner particles to compose a print. Figure 1 is an simplified illustration of cross sections with various amount of toner coverage on paper substrate. Except for the uncoated paper, we can assume that the roughness on the surface of the paper is negligible. Hence, when toner particles begin to adhere on a paper surface, the profile of the surface becomes rougher. This results in the reduction of measured gloss for paper with medium and high gloss. However, when a significant amount of toner particles are laid down on the paper surface, gaps between tone particles begin to disappear, which results in smoother surface. This, in turns, increases gloss. Nonetheless, because the reflectance coefficient of toner particle is often greater than matte-coated paper, the resulted gloss is usually monotonically increasing with respect to the amount of toner. The measured gloss relative to the amount of toner coverage is therefore at least a quadratic polynomial. Furthermore, we assume that the gloss is a weighted average of different toner as following:

$$g_{model} = \sum_{i=1}^{4} w_i g_i \qquad (9)$$

where

$$g_i = a_0^i + a_1^i p_i + a_2^i p_i^2 \qquad (10)$$

$$w_j = p_j / \sum_{i=1}^{4} p_i. \qquad (11)$$

The unknown coefficients $[a_0^i \ a_1^i \ a_2^i]^T$ can be obtained by a least square solution from each channel.
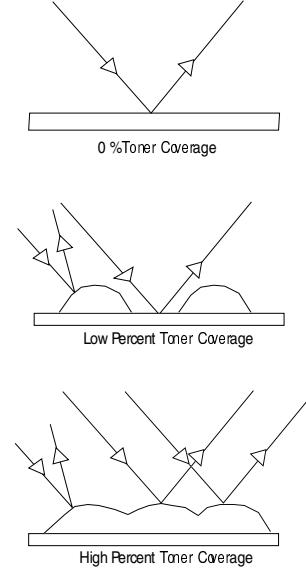

Figure 1: *Simplified illustrations of cross sections with various amount of toner coverage*

3.2. Support Vector Identification

Let $G \in R^{s \times m}$ represent the measured gloss, where there exists s patches for each print and m total prints are used in the analysis. Assuming $\hat{G}_{qm} \in R^{s \times m}$ specifies gloss values predicted by the previous quadratic mixture model, we then adopt the singular value decomposition, *SVD*, to $G - \hat{G}_{qm}$ such that

$$G_r = G - \hat{G}_{qm} = U_r S_r V_r^T. \qquad (12)$$

The range space, $R(G_r)$, is spanned by the columns of U_r, and the diagonal elements of S_r are the square root of eigenvalues of $G_r G_r^T$. It has been shown that *SVD* is the optimal linear projection operator for maximal signal energy concentration on a subspace. Hence, we can assume that the subspace, $[u_r^1 \ u_r^2 \cdots u_r^k]$, where $k \ll m$, is sufficient to approximate the original signal, and the remaining column vectors of U_r contain mainly noise. In our experiment, we found that the first two column vectors of U_r already contains the majority of the energy in G_r. Hence, we propose to apply the *SVR* algorithm on u_r^1 and u_r^2 respectively. Let SV_1 and SV_2 represents the identified support vectors for u_r^1 and u_r^2, and the selected patches, S_p, is the union of SV_1 and SV_2, i.e.:

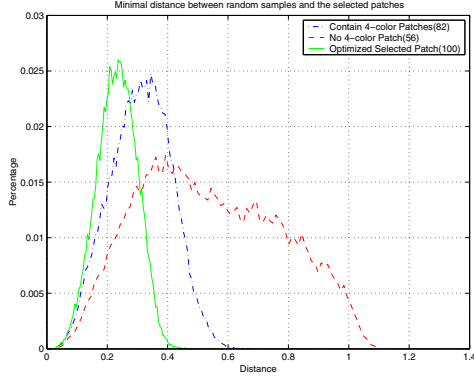$$S_p = \bigcup_{i=1,2} SV_i. \qquad (13)$$

Figure 2: *Histogram of the minimal distance between random samples and selected patches. Red line is derived from 8 color ramps; Blue line is derived by adding 26 near-neutral patches; Green line represents histogram based on the clustering result.*
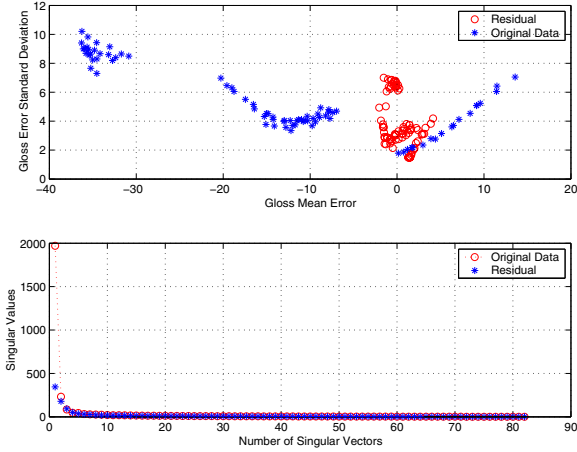

Figure 3: *Summary of the original data and the residual after subtracting the quadratic mixture model prediction*

4. Experiment Results

Four types of paper are selected in this experiment: Enso-4CC Silk, Sappi-Tech Lustro Laser, and Chromcoat 12Pt. Their paper 60-degree gloss readings before printing are 6.8, 35 and 60 respectively.

Before applying the proposed algorithm, we notice that the measured gloss, g, has to satisfy the following constraint: $0 \leq g \leq 100$. Hence, the Probit and inverse Probit transform are adopted as the first and the last operation such that the estimated gloss meets this constraint. Figure 2 illustrates the histogram of the minimal distance between 5000 random points to the selected patches. Three selections are used: one contains 8 color ramps, *C,M,Y,K,R,G,B and 3-Color Neutral*, the second selection includes all noted color ramps and 28 randomly selected near-neutral patches,
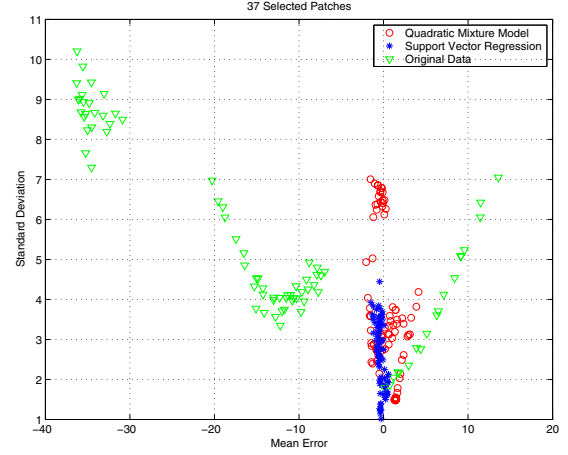

Figure 4: *Comparison between the original data, the residual and the error with 37 patches*

and the last set contains all noted color ramps as well as 42 patches via progressively clustering neighboring sample points into a new sample. It is obvious that 8 color ramps only, 56 patches in total, does not offer sufficient sampling because there exists regions with very few sample points. This problem is drastically reduced via adding near-neutral patches. We further optimized the sampling grid by using a complete-link clustering algorithm, which is also shown in figure 2.

We choose the *radial basis function* as the nonlinear kernel in the *SVR* algorithm, and it has the following form [7,8]:

$$K(x,y) = e^{-u\|x-y\|^2} \tag{14}$$

where u is a scaling factor. We found that $u = 1.4$ reaches a good compromise between offering global and local information.

Figure 3 provides the information of the original data and the residual G_r up to degree two. It clearly show that the mean of G_r after subtracting the prediction by the quadratic mixture model is approximately zero for the adopted printing processes and selected types of paper. Moreover, the first singular value is significantly reduced comparing between the original data and the residual. This means that the proposed quadratic mixture model is able to capture the overall trend of the measured gloss for various types of paper. Figure 4 and 5 illustrate estimation error for all patches based only on 37 and 56 selected patches respectively. It shows that the patches identified by the proposed algorithm further improve the estimation error with increasing number of patches. Nonetheless, the standard deviation of estimation error will not reach zero because of the measurement uncertainty and the estimation ability imposed by the chosen kernel function.
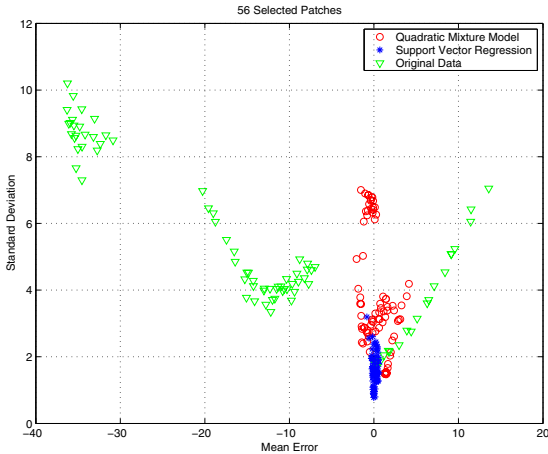
Figure 5: *Comparison between the original data, the residual and the error with 56 patches*
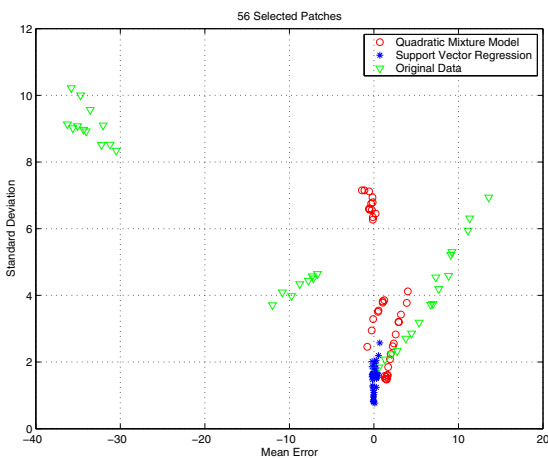

Figure 6: *Generalization testing result by using 56 patches*

38 prints from three types paper, Enso-4CC Silk, Sappi-Tech Lustro Laser and Chromcoat 12pt, are selected as the test set, and we only choose the identified patches to build a gloss regression model for each print. Figure 6 demonstrates that the regression model based on 56 patches is also able to generalize to unseen data.

5. Conclusion

By combining the assumed a priori quadratic mixture model with the *SVR* algorithm with *1-Norm*, the proposed selection algorithm is able to find important samples to build a accurate regression model for various printing processes and paper types. We plan to extend this study to other printing and fusing processes.

6. References

1. C. Jeffrey Wang, Differential Gloss in Electrophotography, **IS&T NIPS 15**, pp. 406-407, (1999).
2. Yee Ng, Chunghui Kuo and C. Jeffrey Wang, Gloss Uniformity Attributes for Reflection Images, **IS&T NIP17**, pp. 718-722, (2001).
3. R. Hunter and R. W. Harold, The Measurement of Appearance, 2nd Ed., **Wiley**, (1987).
4. F. W. Billmeyer and F. X. D. O'Donnell, Visual Gloss Scaling and Multidimensional Scaling Analysis of Painted Specimens, **Color Research and Application**, Vol 12, No 6, pp. 315-326, (1987).
5. G. Ward, Measuring and Modelling Anisotropic Reflection, **Computer Graphics**, Vol 26, No 2, pp. 265-272, (1992).
6. S. G. Mallat, A Wavelet Tour of Signal Processing, 2nd Ed., **Academic Press**, (1999).
7. N. Christianini and J. Shawe-Taylor, Support Vector Machines and other kernel-based learning methods, **Cambridge**, (2000).
8. V. Vapnik, Statistical Learning Theory, **John Wiley**, (1998).
9. O. L. Mangasarian and D. Musicant, Large Scale Kernel Regression via Linear Programming, **Data Mining Institute Technical Report**, (August 1999).
10. A. Smola and B. Schölkopf, A Tutorial on Support Vector Regression, **NeuroCOLT**, (1998).
11. A. Smola, B. Schölkopf and G. Rätsch, Linear Programs for Automatic Accuracy Control in Regression, **ICANN**, pp. 575-580, (1999).
12. V. Vapnik, S. Golowich and A. Smola, Support Vector Method for Function Approximation, Regression Estimation and Signal Processing, **NIPS 9**, (1997).

7. Biography

Chunghui Kuo received his Ph.D in Electrical and Computer Engineering from University of Minnesota and joined *NexPress* since 2001. His research interest is in image processing, image quality and neural network applied in signal processing. He is a member of IEEE signal processing society and *SPIE*.

Yee S. Ng is a Chief Engineer of *NexPress* since 1998. He was a Project Chief Engineer and Science Associate at *Eastman Kodak* Company before that. He received his Ph.D in Physics from Pennsylvania State University and joined Kodak Reserach Laboratory in 1980. His research interests are in image quality, image processing, Electrophotographic processes, electronic Writer and Image Data Path design. He was a Kodak Distinguished Inventor and holds more than 80 U.S. Patents. He received the Carlson Memorial Award in 2000 from *IS&T*.

C Jeffrey Wang received a MS degree from Imaging Science of RIT in 1987. He worked at RITRC between 1987 and 1996. Had joined *Eastman Kodak* later in 1996. He has been working at *NexPress* as a Senior Scientist since 1998. Has published in *IS&T* and *TAGA* proceedings.